Italian Journal of Pediatrics

RESEARCH

Open Access

SVseq discloses the genomic complexity of different prenatal, de novo, apparently balanced chromosome rearrangements detected by CMA and karyotype

Shengfang Qin[1*], Xueyan Wang[1], Chun Chen[1], Jin Wang[1], Zhuo Zhang[1], Yan Yin[1] and Xiangyou Leng[1]

Abstract

Background Balanced chromosomal rearrangements (BCRs) are common structural variations (SVs), but only a small number of individuals with BCRs exhibit abnormalities. To better understand the different phenotypes in children diagnosed with BCRs during the prenatal period, we plan to thoroughly investigate the SVs and evaluate their pathogenicity in five children with BCRs.

Methods Five children with BCRs detected through karyotyping and chromosome microarray analysis (CMA) during prenatal diagnoses were analyzed using SVseq technology. A mate-pair library was sequenced on the DNBSEQ-T7 platform. Copy number variations (CNVs) and SVs were then analyzed with paired-end sequencing files. Furthermore, we performed whole-genome sequencing (WGS) on case 4 at a coverage rate of 30X. The pathogenicities of the findings were evaluated according to the American College of Medical Genetics (ACMG) guidelines. Clinical examinations and follow-up assessments were also carried out for these children.

Results The results from the SVseq analysis indicated the presence of BCRs in two cases, while the other three exhibited complex chromosomal rearrangements (CCR). Overall, the SVs identified in all five children led to gene disruptions. Cases 1, 2, 3, and 5 affected either an autosomal recessive (AR) gene or a non-loss-of-function (non-LOF) autosomal dominant (AD) gene; notably, no abnormal phenotypes were observed in these four cases during the follow-up period. In contrast, Case 4 involved a pathogenic disruption of the *CYLD* gene and showed clinical abnormalities, including developmental delays in intelligence, language, and motor skills. Additionally, this case was analyzed using WGS (30X), excluding other pathogenic or likely pathogenic SNVs/Indels that could explain the patient's abnormal phenotype.

Conclusion The SVseq method has a higher positive detection rate for BCRs than conventional techniques. It is crucial to provide BCR individuals, especially fetuses, with SV validation, genetic counseling, and clinical evaluation.

Keywords Structural variation, Balanced chromosome rearrangement, Complex chromosome rearrangement, SVseq

Background

Balanced chromosomal rearrangements (BCRs) are relatively common structural variations in clinical settings. The estimated incidence of BCRs in the general population is about 0.2% to 0.5% [1, 2], and in newborns is approximately 3 per 1,000 [3]. BCR carriers usually present normal phenotypes; however, a small percentage

*Correspondence:
Shengfang Qin
qinshengfang@126.com
[1] Department of Medical Genetics and Prenatal Diagnosis, Sichuan Provincial Women's and Children's Hospital, Chengdu, Sichuan 610045, China

may exhibit abnormal. Jacobs PA reported that 6% of prenatal patients with BCRs show abnormal phenotypes [4]. Furthermore, 30% to 50% of newly identified BCRs are estimated to be abnormal phenotypes [5, 6]. Complex chromosomal rearrangements (CCRs) with three or more breakpoints are associated with a higher prevalence of abnormal phenotypes than simple BCRs, and the more chromosomes or breakpoints involved, the greater probabilistic the abnormality and the more severe the symptoms [7].

Conventional methods for identifying BCRs have their limitations. Karyotyping has low resolution and is unable to detect submicroscopic rearrangements. Chromosomal Microarray Analysis (CMA) can identify abnormal increases or decreases in genome copy number but cannot detect balanced rearrangements such as inversions or translocations. Furthermore, whole exome/whole genome sequencing (WES/WGS) is constrained by short-read lengths and is ineffective in detecting structural variation, particularly long-distance rearrangements. Therefore, clinical detection of SVs, such as BCRs, inversions, and CCRs, remains challenging.

The phenotypic normality of fetuses with BCRs, identified through CMA and karyotype analysis during prenatal diagnosis, remains uncertain at birth. To thoroughly assess the pathogenicity of BCRs and potential clinical implications, we analyzed copy number variations (CNVs) and SVs in five children who had BCRs identified prenatally through karyotype and CMA. For this analysis, we utilized SVseq technology. Additionally, we conducted clinical examinations and follow-up assessments with these children after their birth.

Methods

Subjects

Five children, four boys and one girl, were aged between 105 days and four years and three months. We conducted clinical examinations and routine follow-ups for childcare. Four children(Case 1, 2, 3, 5) appeared apparently healthy, while the other (Case 4) exhibited an abnormality. During prenatal diagnosis, these fetuses were diagnosed with de novo BCRs by karyotype and CMA same as previous methods [8], including de novo balanced chromosome translocations (BCTs) in four cases and BCRs in one case (details in Table 1). Additionally, their ultrasound examinations did not show any abnormalities.

Case 4 was a three-year-old girl who was stunted, short, and thin. Her height was 89.6 cm (5 th percentile) and her weight was 11.8 kg (5 th percentile). She presented with distinctive facial features, including a prominent forehead, wide-set eyes, sunken eye sockets, a flat nose bridge, a short nose-lip-distance, thin and short eyebrows, and epicanthus. Additionally, she had patches of thin and thick hair on her back. Her mother stated that the child tended to scratch her face, leading to visible scratches. The girl experienced delayed language development; her speech was unclear, primarily consisting of short words such as"dad"and"mom."Furthermore, she faced difficulties with feeding, often consuming only small amounts of food, and she had an allergy to eggs.

She began walking at the age of 2. By age 3, she could walk slowly and smoothly and run unsteadily but could not jump. Laboratory tests indicated normal thyroid function, blood cell counts, and a 25-OH vitamin D level. Her insulin-like growth factor 1 (IGF-1) level was 62.70 ng/mL (reference range: 18–172 ng/mL), while insulin-like growth factor binding protein 3 (IGFBP-3) level was 5.18 μg/mL (reference range: 0.9–4.3 μg/mL). Iron metabolism tests showed normal levels of ferritin, serum iron (Fe), and transferrin (TRF); her iron saturation was 17.6%, below the reference range of 20–55%. The total iron binding capacity (TIBC) was 73.7 μmol/L, higher than the reference range of 45–72 μmol/L. Three years ago, the mother underwent a prenatal diagnosis at 18 weeks and 4 days due to an increased nuchal translucency (NT) value of the fetus. Karyotype analysis of the amniotic fluid cells showed de novo BCRs, while no abnormalities were found in the chip analysis using the 180 k aCGH + SNP Chip (Agilent Technologies). A cesarean section was performed at 39 weeks after the mother experienced a decrease in amniotic fluid at 37 weeks. Neither the mother nor the father has a family history of genetic disorders or consanguinity; however, the mother had a history of paint exposure before and during her pregnancy, and the father did not quit smoking.

Specimen preparation

Genomic DNA was extracted from EDTA-Na2 anticoagulated blood using the QIAamp DNA Mini Kit (QIAGEN, Germany), following the manufacturer's instructions. The DNA was assessed for quality, with a concentration exceeding 20 ng/μL and an absorbance ratio (A260/A280) between 1.8 and 2.0, as measured with a Nanodrop 1 C ultraviolet spectrophotometer (Thermo Fisher Scientific, USA).

All procedures in this study followed the principles of the Helsinki Declaration and received approval from the institutional review board of Sichuan Provincial Women's and Children's Hospital. Informed consent was obtained from all guardians before the collection of clinical data and samples.

SVseq analysis

We analyzed the genomic DNA of five BCR blood samples using SVseq. First, we created a mate-pair library with the MP Library Prep Kit from GeneTech Co., Ltd,

Table 1 SVseq results, actual karyotype, pathogenicity, and clinical follow-up of 5 BCRs fetuses

Case	Gender	Years old	Karyotype(G-band)	CMA results	Clinical phenotype	SVseq indication	SVseq results	Actual Karyotype (Karyotypic complex format)	Conclusion	Pathogenicity
1	M	four years	46,XY,t(1;9)(p31;q31)dn	N	N	BCT(dn)	SVseq results showed the translocations of chromosomes 1 and 9. The karyotype is t(1;9)(1p22.2;9q31.1). Meanwhile, the translocation fragment of 1p22.2-1p22.1 (chr1:91,139,281–92,220,091) was inverted. The structural variation involved three breakpoints, and the breakpoint in 9q31.1(chr9:102,880,213) destroyed the *INVS* gene associated with AR infant nephropathy type 2	46,XY,t(1;9)(9q34.3→9q31.2::1p22.1→1p22.2::1p22.1→1q34;9p24.3→9q31.1::1p22.2→1p36.33) (see Fig. 1)	CCR	VUS
2	M	four years and three months	46,XY,t(4;8)(q21;q24.1)dn	N	N	BCT(dn)	SVseq showed balanced translocations of chromosomes 4 and 8. The karyotype is t(4;8)(q21.21;q24.12). The breakpoint in 8q24.12 (chr8:120,829,658) disrupts the protein-coding gene *TAF2*, associated with AR intellectual disability type 40	46,XY,t(4;8)(4p16.3→4q21.21::8q24.12→8q24.3;8p23.3→8q24.12::4q21.21→4q35.2) (see Fig. 2)	BCT with the destruction of AR gene	VUS
3	M	four years and three months	46,XY,t(12;13)(p11.23;q12)dn	N	N	BCT(dn)	SVseq showed balanced translocations of chromosomes 12 and 13. The karyotype is t(12;13)(p12.1;q12.11). The breakpoint at 12p12.1 (chr12:252,140,644) disrupted the protein-coding gene *IRAG2*. The breakpoint in 13q12.11 (chr13:22,256,106) disrupted the AD gene *FGF9,* related to multiple synostoses syndrome 3	46,XY,t(12;13)(12q24.33→12p12.1::13q12.11→13q34;12p13.33→12p12.1::13q12.11→13p13) (see Fig. 2)	BCT with the destruction of protein-coding gene and AD gene	VUS

Table 1 (continued)

Case	Gender	Years old	Karyotype(G-band)	CMA results	Clinical phenotype	SVseq indication	SVseq results	Actual Karyotype (Karyotypic complex format)	Conclusion	Pathogenicity
4	F	three years	46,XX,ins(2;16)(p13;q12q24),t(2;5)(q23;p15.1),t(2;8)(p13;p22)dn	N	A three-year-old girl was stunted, short, and thin, measuring 89.6 cm in height (5 th percentile) and weighing 11.8 kg (5 th percentile). She had a prominent forehead, wide-set eyes, sunken eye sockets, a flat nose bridge, a short distance between her nose and lip, thin and short eyebrows, and epicanthic folds. Additionally, her face had many tiny scratches and thin and short hair on the surface of the back	BCT(dn)	The SVseq result showed the CCR involved four chromosomes, including the complex rearrangement of chromosome 12 itself accompanied by two microdeletion fragments and complex translocations among chromosomes 2, 5, and 16. The chr2: 65,629,712 broke the *SPRED2* gene, and the chr16: 50,800,833 breakpoint destroyed the *CYLD* gene with a haploinsufficiency effect	(see Fig. 3,Fig. 5)	CCR	P
5	M	105 days	46,XY,inv(6)(p11.2q21),?ins(7;6)(p15;q21q23) dn	N	N	BCRs(dn)	The SVseq showed the complex rearrangement of 14 breakpoints on chromosomes 6 and 7 involving protein-coding genes of *C1GALT1*, *MIOS*, *RPA3*, *TRAM2*, and *DSE*. The *DSE* gene is associated with AR Ehler-Danlos syndrome type 2 muscle contraction (OMIM: 615,539)	(see Fig. 4)	CCR	VUS

M male, *F* female, *dn* de novo, *N* normal, *BCT* balanced chromosome translocation, *BCRs* balanced chromosomal rearrangements, *CCR* complex chromosomal rearrangements, *P* pathogenicity, *VUS* variants of uncertain significance

Shanghai, China [9, 10]. Afterward, we performed sequencing in PE150 mode on the DNBSEQ-T7 platform (MGI) with an average target coverage of >5x. After obtaining the raw data, we compared high-quality paired reads with the NCBI Human reference Genome (GRCh37) using BWA, following the removal of sequencing splice-containing and low-quality reads. Pair-reading was employed to identify all chromosome CNVs and SVs.

WGS (30X) analysis

The data was analyzed using the Verita Trekker® mutation site detection system and the Enliven® mutation site annotation interpretation system, developed independently by Berry Gene. Single Nucleotide Variants (SNVs) and Insertions/Deletions (InDels) were screened based on clinical phenotypes or genes associated with specific diseases, utilizing public databases such as HPO, OMIM, and GHR. The analysis followed the guidelines established by the American Society for Medical Genetics and Genomics (ACMG) [11].

Sanger Sequencing and breakpoints validation

To pinpoint the exact location of the breakpoints, we designed gene-specific primers using Primer 6 based on the initial breakpoint location obtained from SVseq (see Table 2). These primers were synthesized by Shenggong Biotechnology Co., LTD (Shanghai). The PCR products were subsequently sequenced using Sanger sequencing with an ABI-A3130 gene analyzer. The exact breakpoints were identified by comparing both ending sequences of the breakpoints in the gene bank.

Pathogenicity assessment and clinical follow-up

The pathogenicities of structural variation were assessed based on the ACMG guidelines [11]. We performed clinical examinations and follow-ups for the children involved in the study. The follow-up periods ranged from a minimum of 100 days to a maximum of 4 years and 3 months. Clinical phenotypes were evaluated thoroughly using clinical assessments and relevant laboratory results related to childcare indicators.

Results

Results of structural variation detection

The SVseq test provided additional insights into the chromosome karyotype of the five BCR children, as shown in Table 1. Among these cases, three (Case 1, Case 4, and Case 5) were classified as CCRs, as illustrated in Figs. 1, 3, and 4. The remaining two cases were balanced translocations between chromosomes 4 and 8 (Case 2, Fig. 2a), and chromosomes 12 and 13(Case 3, Fig. 2b), resembling their karyotypes.

In Case 1 (Fig. 1), the SVseq results revealed translocations involving chromosomes 1 and 9. Specifically, the translocated fragment of chromosome 1, spanning from 1p22.2 to 1p22.1 (chr1:91,139,281–92,220,091), was inverted. This structural variation involved three breakpoints, and one of the breakpoints located at 9q31.1 (chr9:102880213) disrupted the *INVS* gene, which is associated with autosomal recessive (AR) infant nephropathy type 2.

In Case 4, the karyotype revealed a complex, balanced rearrangement involving four chromosomes, denoted as 46, XX, ins(2;16)(p13;q12q24),t(2;5)(q23;p15.1),t(2;8)(p13;p22) dn (see Fig. 3a). The SVseq results indicated that the CCRs involved four chromosomes, including a complex rearrangement of chromosome 12 accompanied by two microdeletion fragments (chr12: 33204296–33214293, chr12: 62733777–62963184). Additionally, there were complex translocations among chromosomes 2, 5, and 16 (refer to Fig. 3b). Notably, the breakpoint at chr2: 65629712 affected the *SPRED2* gene (OMIM: 609292), which is associated with AR Noonan syndrome type 14 (OMIM: 619745). Furthermore, the breakpoint at chr16: 50800833 disrupted the *CYLD* gene (OMIM: 605018), which is linked to haploinsufficiency effects related to several autosomal dominant syndromes, including Brooke's Spiegler syndrome. The affected girl's facial features (illustrated in Fig. 3c) included a

Table 2 Sequence of Sanger sequencing primers for verifying breakpoints in gene regions

Case	Location	Forward primer	Reverse primer	Gene involved
1	chr9-chr1, 102880213–91134406	TGAGACAGAGTCTCGCTCT	GCTGTGAATTCAACACTCAGGT	*INVS*
2	chr8-chr4, 120829658–82301340	CCTGAGACAGAGGTCCTTACG	AGGATCAATGATTTAGAGGCTGCT	*TAF2*
3	chr13-chr12, 22256106–25214064	GACTCATGTGTGTCTGCCCA	ACCCACAACCCAATTTTCCTTC	*FGF9*
4	5'chr2:155914861–155915361(Reverse), 3'chr2:65629712–65630212	GGAACACAGGTTTCATCACCAG	CACGTGAACATGTTCTAGGGC	*SPRED2*
4	5'chr16:50800270–50800770, 3'chr5:30709364–30709864(Reverse)	ATACATTCTGTAAGGCTGCCA	GCTGATCTGTCCAAGGTTTTG	*CYLD*
5	chr6:52438625-chr6:116729330	TCCTGGCTGAAGAGCGGGTAAC	GTTAGCTCACAAGTTTGGCTCAT	*DSE*

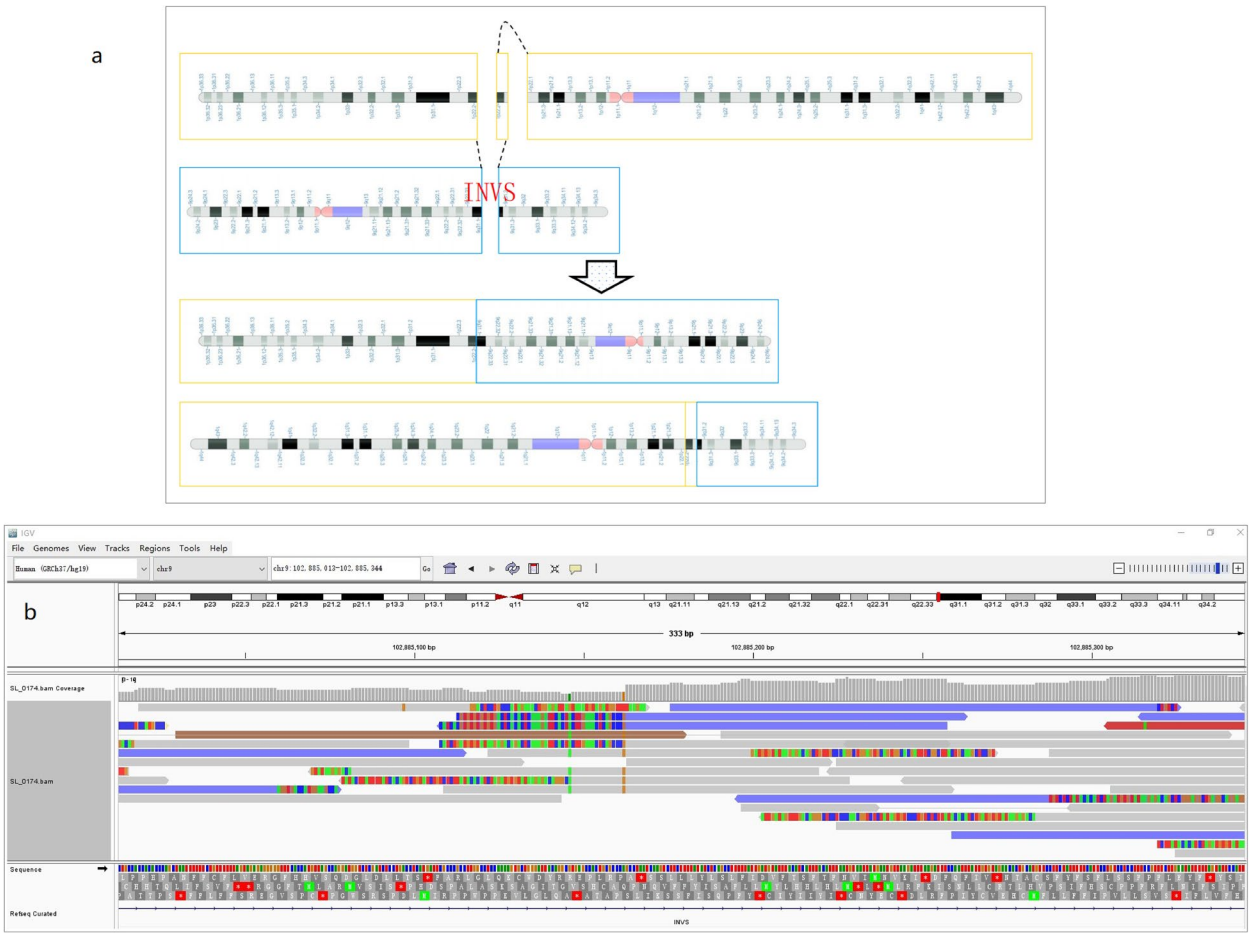

Fig. 1 Complex chromosomal rearrangements (CCR) detected by SVseq in Case 1. **a** This schematic diagram illustrates the CCR identified by SVseq in Case 1. The results of the SV sequencing indicated translocations between chromosomes 1 and 9, resembling the karyotype of t(1;9)(1p22.2;9q31.1) (not shown). Additionally, the translocation fragment of 1p22.2-1p22.1 (chr1:91,139,281–92,220,091) was inverted. This structural variation involved three breakpoints, with one at 9q31.1 (chr9:102880213) disrupting the *INVS* gene, which is associated with AR infant nephropathy type 2. **b** The Integrated Genomics Viewer (IGV) visualization of the BAM file shows the fragments disrupting the protein-coding gene *INVS*. The colorful regions represent the mismatched sequences of the target regions

prominent forehead, wide-set eyes, sunken eye sockets, a flat nose bridge, a short distance between the nose and lip, thin and short eyebrows, and epicanthus.

The karyotype described as 46, XY, inv(6)(p11.2q21),?ins(7;6)(p15;q21q23) indicates a complex, balanced rearrangement involving two chromosomes in Case 5 (Fig. 4a). The SVseq results (Fig. 4b) revealed a complex rearrangement comprised of 14 breakpoints on chromosomes 6 and 7, affecting the protein-coding genes *C1GALT1, MIOS, RPA3, TRAM2,* and *DSE*. Notably, the *DSE* gene is linked to AR Ehlers-Danlos syndrome type 2, associated with muscle contraction (OMIM: 615539).

All five cases destroyed the relevant genes. The junctions were confirmed through Sanger sequencing. The verification results for Case 4, which involved the genes *SPRED2* (Fig. 5a) and *CYLD* (Fig. 5c), were consistent with the breakpoints identified by WGS (30X), as shown in Figs. 5b and d. Furthermore, the WGS (30X) results for Case 4 ruled out pathogenic or likely pathogenic variants in SNVs and Indel-related genes that could account for the patient's abnormal phenotype.

Pathogenicity assessment and clinical follow-up results

The pathogenicity assessment conducted by ACMG indicated that the breakpoint at chr16:50800833 in Case 4 represented a pathogenic variant, which could potentially impact the function of the *CYLD* gene. Consequently, the patient displayed abnormal clinical phenotypes. In contrast, the clinical significance of the other four cases was classified as variants of uncertain significance (VUS), and follow-up results revealed no abnormalities (Table 1).

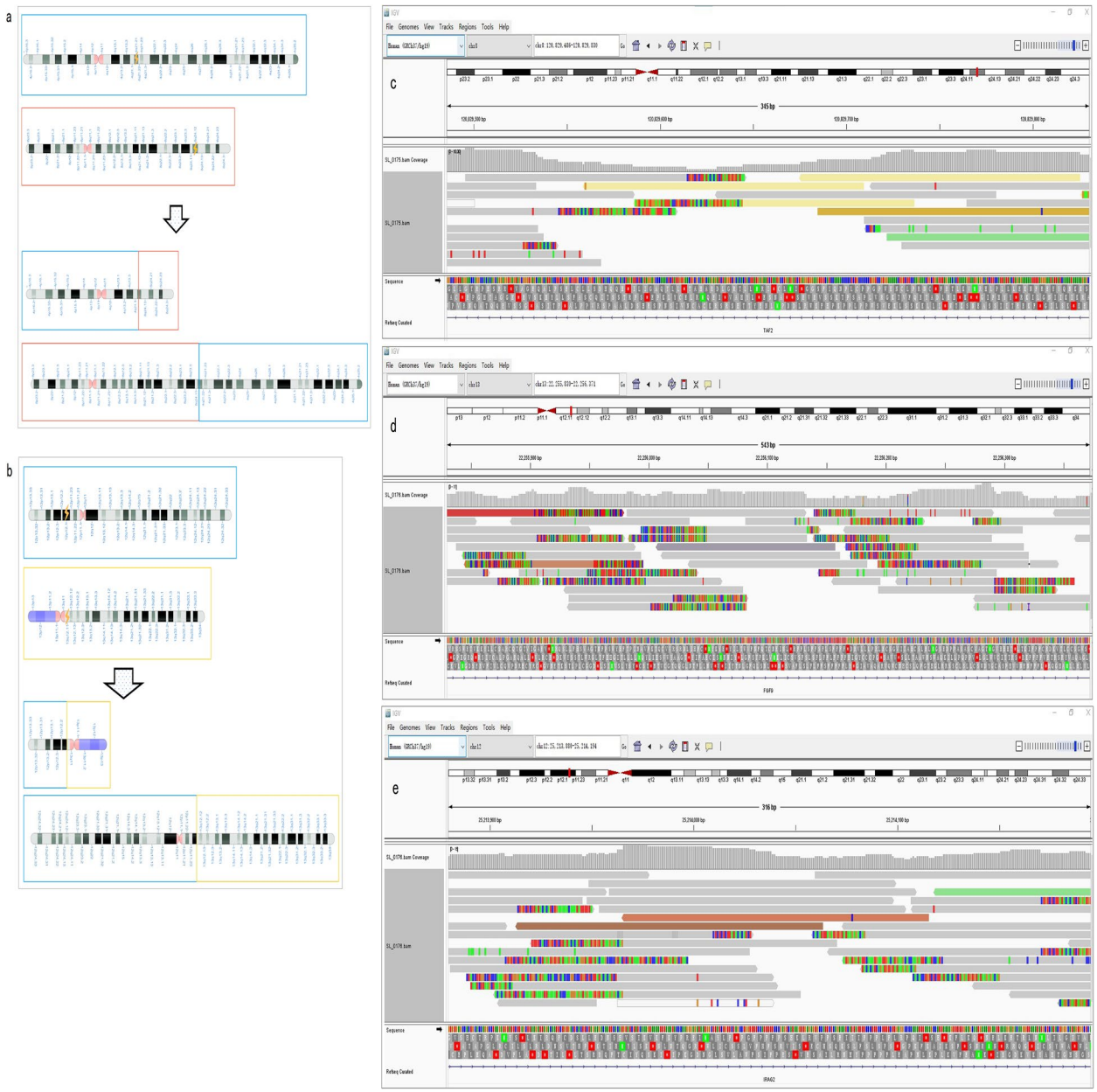

Fig. 2 Balanced translocations determined by SVseq in Cases 2 and 3. This schematic diagram illustrates the balanced translocations identified by SV sequencing in Cases 2 and 3 (Fig. 2a, b). The results revealed balanced translocations between chromosomes 4 and 8 in Case 2 and between chromosomes 12 and 13 in Case 3, which aligns with their respective karyotypes. Figures 2c-e show IGV visualizations of fragments that disrupt the protein-coding genes *TAF2* in Case 2 (Fig. 2c) and *FGF9* and *IRAG2* in Case 3 (Fig. 2d, e)

Discussion

Some patients with BCRs have cryptic imbalances that cannot be identified due to the low resolution of conventional karyotyping, which ranges from 5 to 10 Mb. Consequently, the actual occurrence of chromosomal translocations and inversions is much higher than the estimated rate of 0.16–0.2% reported in G-band karyotype analysis [12]. CMA and CNVseq are more effective in identifying submicroscopic chromosomal imbalances than traditional cytogenetic techniques [13]. The array CGH technique has revealed that about 30–50% of patients present with microdeletions. Both de novo cases (48.5%) and familial cases (28.6%) exhibit these imbalances [14]. Research indicates that CMA technology enhances the detection rate of genetic aberrations in patients with mental retardation (MR) from 5% to

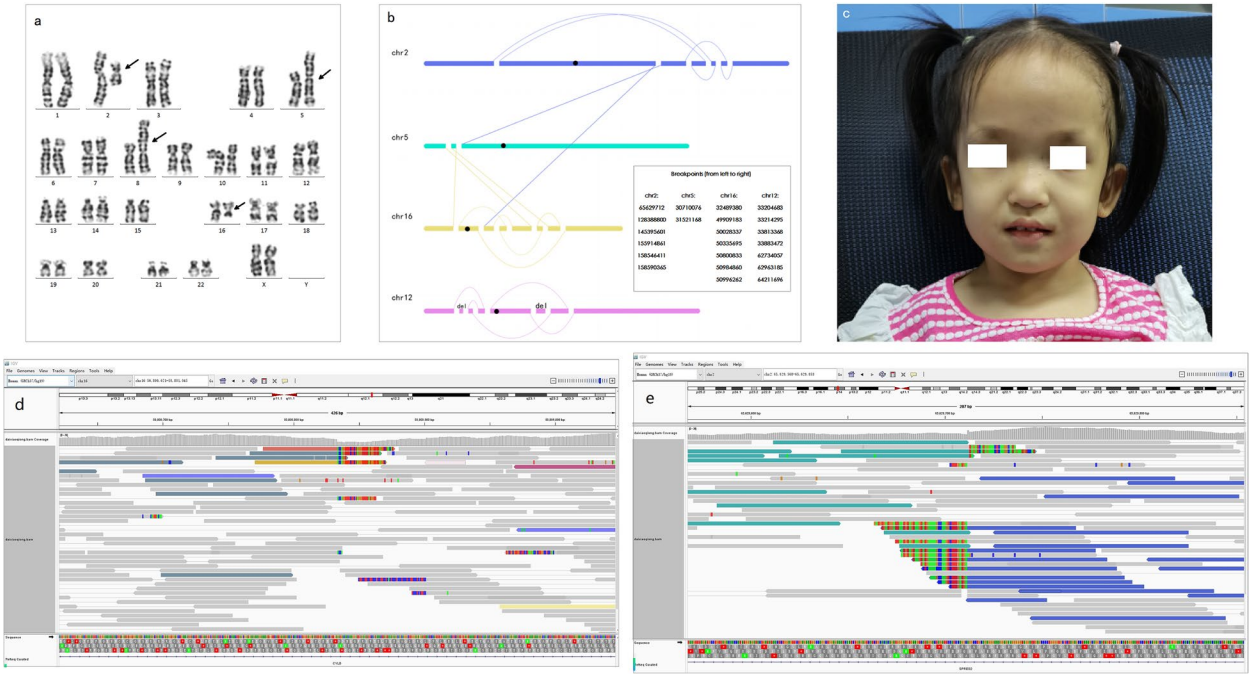

Fig. 3 CCR Identified by SVseq in Case 4. The karyotype and SV result pattern diagram of Case 4 revealed a complex, balanced rearrangement involving four chromosomes, depicted as 46, XX, ins(2;16)(p13;q12q24),t(2;5)(q23;p15.1),t(2;8)(p13;p22) dn (Fig. 3a). The SVseq results further indicated that the chromosomal rearrangements involved four chromosomes. This included a complex rearrangement of chromosome 12, accompanied by two microdeletion fragments (chr12: 33204296–33214293, chr12: 62733777–62963184), as well as complex translocations between chromosomes 2, 5, and 16 (Fig. 3b). The breakpoint on chromosome 2 (chr2: 65629712) affected the *SPRED2* gene (OMIM: 609292), which is associated with AR Noonan syndrome type 14 (OMIM: 619745). Meantime, the breakpoint on chromosome 16 (chr16: 50800833) disrupted the *CYLD* gene (OMIM: 605018), leading to haploinsufficiency. The orientation of the derived chromosomes is indicated by the illustrated line, with breakpoints listed in the lower right corner of the diagram. The affected girl exhibited distinctive facial features (Fig. 3c), including a prominent forehead, wide-set eyes, sunken eye sockets, a flat nose bridge, a short distance between the nose and lip, thin and short eyebrows, and epicanthus. The IGV visualization shows the fragments disrupting the protein-coding genes *CYLD* and *SPRED2* (Fig. 3d, e)

approximately 17% [15]. Shaw-Smith et al. [16] have suggested that unbalanced translocations should be ruled out first when BCR individuals present with an abnormal phenotype. In this study, SVseq detected imbalanced rearrangements not identified by karyotyping or CMA in Cases 4 and 5.

For balanced rearrangements, such as balanced translocations and inversions, CMA/CNVseq is unable to detect these changes [17]. Therefore, we utilize SVseq technology, based on the mate-pair strategy [18, 19], to comprehensively gather information about rearrangements, including balanced translocations and inversions [20]. SVseq offers a higher detection rate for chromosomal structural variations comparing traditional methods like CMA/CNVseq [10, 21], especially for cryptic chromosome rearrangements, complex rearrangements, and balanced rearrangements that cause gene destruction [22]. However, SVseq has limitations in detecting highly repetitive regions, Robertsonian translocations, and inter-arm inversions of chromosome 9. In case 4 of this study, SVseq failed to identify a breakpoint on chromosome 8, and IGV software did not detect a similar breakpoint in the BAM file generated from WGS(30X). Meanwhile, karyotype analysis indicated a translocation on chromosome 8. We hypothesize that the junction lies within the telomere region at 8pter, where highly repetitive sequences are not detectable by short-read sequencing methods. This situation underscores the importance of jointly analyzing multiple technologies.

Balanced rearrangements can also influence gene function through various mechanisms, such as dose-sensitive gene disruption [23], the formation of new fusion genes, the effects of structural disruption on gene location [24], or the exposure of recessive variants [25]. In our study, four cases—Case 1, Case 2, Case 3, and Case 5—showed evidence of gene destruction. However, no abnormal phenotypes were observed during the follow-up period. This lack of observed abnormalities may be linked to the disruption of one allele of the AR gene or the presence of non-loss-of-function alleles of the AD gene. The pathogenic effects of genes or their regulatory elements caused by a translocation might not be

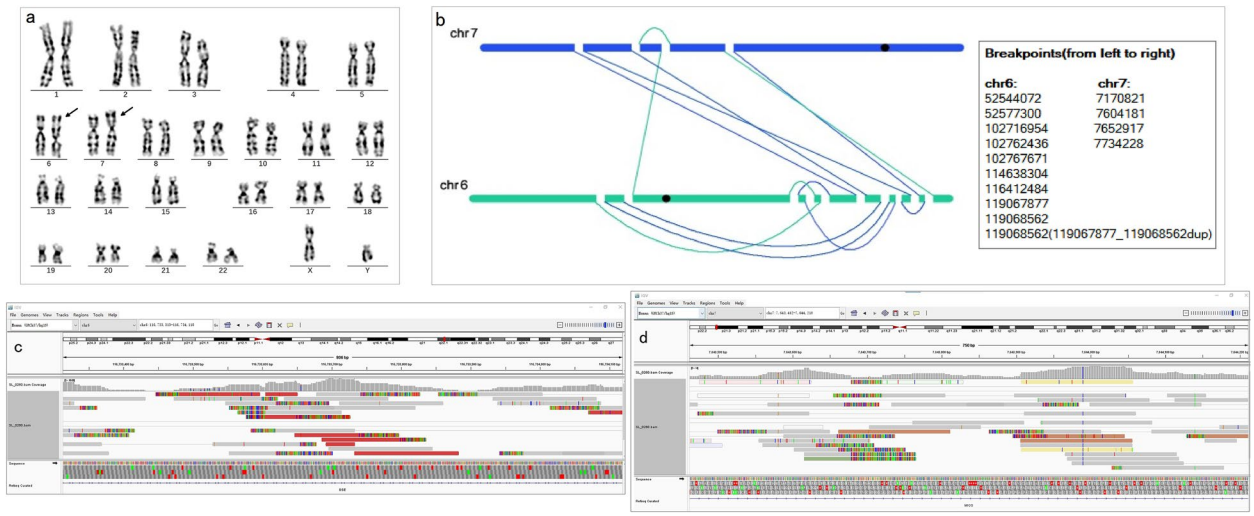

Fig. 4 CCR detected by SVseq in Case 5. This model diagram illustrates the SV detection results in Case 5. The karyotype for Case 5 was identified as 46, XY, inv(6)(p11.2q21),?ins(7;6)(p15;q21q23), indicating a complexly balanced rearrangement involving four chromosomes (see Fig. 4a). The SVseq results (Fig. 4b) revealed 14 breakpoints on chromosomes 6 and 7, affecting several protein-coding genes, including *C1GALT1*, *MIOS*, *RPA3*, *TRAM2*, and *DSE*. Notably, the *DSE* gene is associated with AR Ehlers-Danlos syndrome type 2, which impacts muscle contraction (OMIM: 615539). The derived chromosomes 6 and 7 are linked by green and blue lines, respectively, with a list of breakpoints provided on the right side. The IGV visualization displays fragments disrupting the protein-coding genes *DSE* and *MIOS* (Fig. 4c-d)

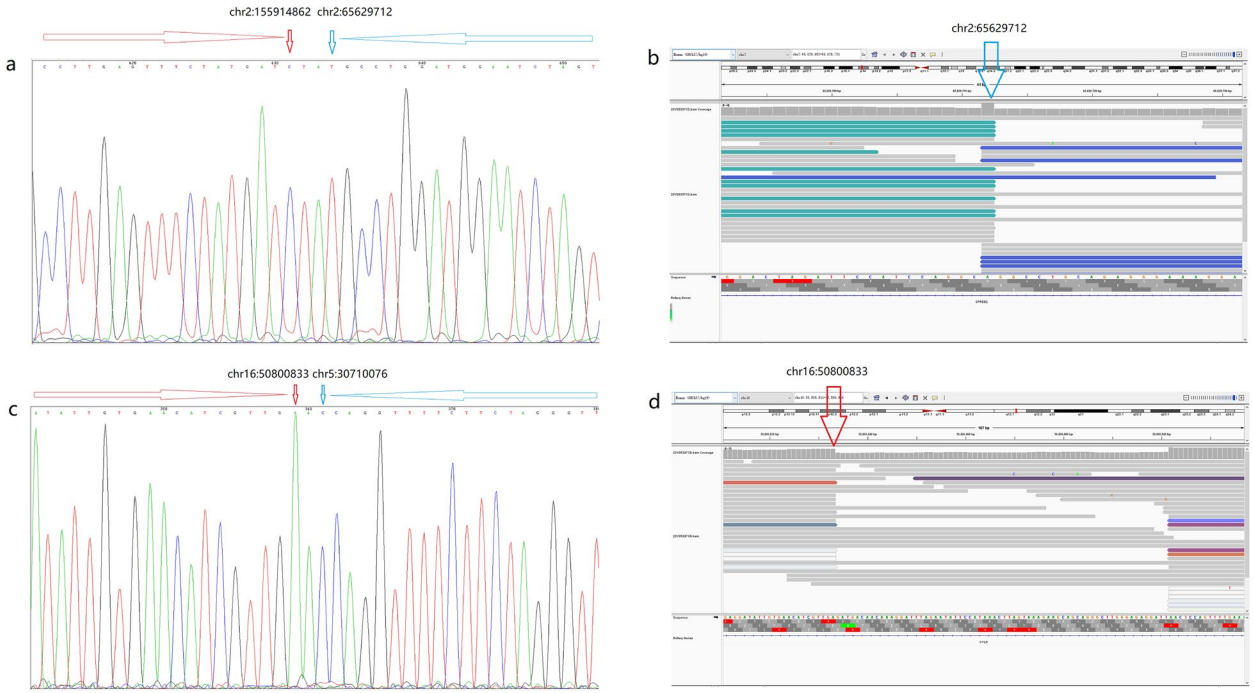

Fig. 5 The Sanger and IGV diagram of breakpoints in *SPRED2* and *CYLD* genes in Case 4. The blue arrow above (**a**, **b**) indicates the breakpoint in the *SPRED2* gene (chr2:65629712), while the red arrow below (**c**, **d**) illustrates the breakpoint in the *CYLD* gene (chr16:50800833)

apparent at birth unless there are specific pathological conditions with clear clinical features. Halgren et al. demonstrated that after an average follow-up of 17 years, the risk of neurodevelopmental and/or neuropsychiatric disorders for de novo translocations identified during pregnancy—with regular first-trimester screening

and ultrasound—rose to 27% in a study of 41 individuals, a significantly higher frequency than a matched control group [26]. In the subsequent follow-up, we will continue to evaluate the risk of neurodevelopmental and/or neuropsychiatric disorders in these children. In the results from these five cases, several genes exhibited breaks and reconnections, suggesting the possibility of fused genes, although these have not yet been analyzed. Next, we will verify these potential fusion genes and research relevant functions.

Recent advancements in detection methods and higher-resolution imaging have revealed that some cases previously classified as balanced chromosomal rearrangements (BCRs) may be CCR. Most patients diagnosed with de novo balanced CCR shortly after birth present with multiple congenital abnormalities, intellectual disabilities, and developmental delays. However, a few individuals may appear apparently healthy in early life but later face issues such as infertility, recurrent miscarriages, low fertility, oligospermia, or azoospermia in adulthood [27]. The risk of abnormalities increases with the complexity of genome rearrangements, particularly when more chromosomes or breaks are involved. Research indicates that balanced CCR is extremely rare, especially during the prenatal periods. In a retrospective study of 60 cases with a prenatal diagnosis of"balanced"complex translocations, it was found that 27 cases were confirmed as de novo CCR after birth [7]. Additionally, many of these cases were linked to multiple congenital abnormalities, intellectual disabilities, or both. Studies have also shown that some BCR patients have unexpected genomic complexity and instability [28], with additional candidate pathogenic CNVs near the translocation breakpoint [5, 29] or complex rearrangements with multiple breakpoints [30].

In our study, despite the genomic complexity revealed in cases 1, 4, and 5, only case 4 showed the potential genotype–phenotype correlation involving the disruption of the *CYLD* gene. Case 1 exhibited three junctions involving translocation and inversion. Case 5 presented with 14 junctions related to chromosomes 6 and 7. In case 4, a complex rearrangement involving up to 22 junctions was observed on chromosomes 2, 5, 12, and 16. The breakpoint of this case led to the pathogenic disruption of the *CYLD* gene, which had a HI score of 3. The follow-up indicated that the girl in case 4 displayed a significantly abnormal clinical phenotype, primarily characterized by global developmental delays that affected both her motor and language skills, as well as severe intellectual disability. Defects in the *CYLD* gene can cause various syndromes inherited in an autosomal dominant pattern, including Brooke's Spiegler syndrome (BRSS, OMIM 605041), familial cylindromatosis (OMIM 132700), multiple familial trichoepithelioma type 1 (MFT1, OMIM 601606), and frontotemporal dementia with amyotrophic lateral sclerosis type 8 (FTDALS8, OMIM 619132). The first three syndromes are associated with tumors. Given the young age of the patients in this study, no tumor-related clinical phenotypes have been observed so far. However, the serum level of Neuron Specific Enolase (NSE), a marker often linked to tumors, was elevated. It is still uncertain whether this high NSE level indicates a pre-tumor condition, so we plan to continue monitoring it. While FTDALS8 is linked to a phenotype of mental retardation, no cases of infantile-onset similar to that of our patient have been documented. The average coverage rate of SVseq is 5X, which might miss additional SNV/indel. Therefore, we performed additional sequencing using WGS at coverage of 30X, and the result ruled out other pathogenic or likely pathogenic SNVs and indels that could explain the patient's abnormal phenotype. Based on these findings, we hypothesize that the disruption of the CCR, particularly in the *CYLD* gene, is the primary cause of the observed abnormal phenotype. However, it is crucial to investigate further the possibility of potential fusion genes or other pathogenic factors, including epigenetic influences.

For parents, if your child is found to have a de novo BCR or CCR, we recommend that you pursue a comprehensive clinical evaluation and genetic counseling. It is essential to assess the pathogenicity of this structural variation, including whether the observed BCR is indeed a true BCR and whether the breakpoints disrupt any relevant functional genes, even if the genome appears balanced.

Conclusions

The conventional methods currently used for BCR detection have several limitations. The SVseq technique shows a significantly higher positive detection rate for copy number variations (CNVs) and structural variations (SVs) comparing these traditional methods. In our study, among five fetuses previously diagnosed with BCRs through routine prenatal methods, four children showed no abnormalities during the clinical examination and evaluation after birth. However, one child (Case 4) exhibited an abnormal phenotype, including global developmental delays in motor skills, language, and severe mental retardation. Using SVseq, we further analyzed their CNVs and SVs and assessed their pathogenicity according to the ACMG guidelines. Among the findings, four cases (Case 1, 2, 3, 5) were classified as variants of uncertain significance (VUS), while Case 4 displayed a pathogenic structural variation in the *CYLD* gene after excluding other pathogenic or likely pathogenic SNV/Indel that could account for the patient's abnormal

phenotype through whole genome sequencing (WGS) at 30X coverage. The current diagnosis of abnormal BCRs primarily relies on postnatal examinations, making it challenging to accurately assess clinical outcomes in BCR fetuses, particularly for abnormalities not detectable through imaging. Our results highlight the importance of selecting an appropriate detection method to validate the pathogenicity of BCRs identified through standard procedures, especially for fetuses with abnormalities that imaging cannot detect. Additionally, genetic counseling plays a crucial role in identifying potential causes of pathogenicity and predicting clinical outcomes for individuals with BCRs.

Abbreviations

BCRs	Balanced chromosomal rearrangements
SVs	Structural variations
CMA	Chromosome microarray analysis
CNVs	Copy number variations
ACMG	The American College of Medical Genetics
CCR	Complex chromosomal rearrangements
AR	Autosomal recessive
AD	Autosomal dominant
BCTs	Balanced chromosome translocations
SNVs	Single Nucleotide Variants
InDels	Insertions/Deletions
VUS	Variants of uncertain significance
TAD	Topological association domain
WGS	Whole-genome sequencing
IGV	The Integrated Genomics Viewer

Acknowledgements
The authors thank Dr. Hongwei Wang, Feng Zhang, and Huiqing Dai from GeneTech Co., Ltd for the SVseq analysis and thank the families for participating in this study.

Authors' contributions
SFQ contributed to the study's conception and design. XYW performed the clinical data collection and genetic counseling. JW made the follow-up and clinical evaluation. CC, ZZ, and YY proceeded with the relevant experiments. XYL analyzed the experiment results and interpreted the patient data. All authors read and approved the final manuscript.

Funding
This research was funded by the Science and Technology Innovation Fund Project of Sichuan Provincial Women's and Children's Hospital (20240102).

Data availability
The datasets used and/or analyzed during the current study are available from the corresponding author on reasonable request.

Declarations

Ethics approval and consent to participate
Ethics approval was granted by the Institutional Review Board of Sichuan Provincial Women's and Children's Hospital (NO. 20231102–278). The guardians of these children were fully informed and signed informed consent forms before the testing.

Consent for publication
Not applicable.

Competing interests
The authors declare that they have no competing interests.

Received: 21 December 2024 Accepted: 11 May 2025
Published online: 24 May 2025

References

1. Dong Z, Zhang J, Hu P, Chen H, Xu J, Tian Q, et al. Low-pass whole-genome sequencing in clinical cytogenetics: a validated approach. Genet Med. 2016;18(9):940–8.
2. Jonas RK, Montojo CA, Bearden CE. The 22q11.2 deletion syndrome as a window into complex neuropsychiatric disorders over the lifespan. Biol Psychiatry. 2014;75(5):351–60.
3. Jurčenko M, Auzenbaha M, Mičule I, Grīnfelde I, Dzalbs A, Mālniece I. Implication of Genetic Testing and Pregnancy Outcome in a Woman with Unbalanced Translocation t(1;6). Am J Case Rep. 2022;23: e935370.
4. Jacobs PA, Browne C, Gregson N, Joyce C, White H. Estimates of the frequency of chromosome abnormalities detectable in unselected newborns using moderate levels of banding. J Med Genet. 1992;29(2):103–8.
5. De Gregori M, Ciccone R, Magini P, Pramparo T, Gimelli S, Messa J, et al. Cryptic deletions are a common finding in "balanced" reciprocal and complex chromosome rearrangements: a study of 59 patients. J Med Genet. 2007;44(12):750–62.
6. Sismani C, Kitsiou-Tzeli S, Ioannides M, Christodoulou C, Anastasiadou V, Stylianidou G, et al. Cryptic genomic imbalances in patients with de novo or familial apparently balanced translocations and abnormal phenotype. Mol Cytogenet. 2008;1:15.
7. Madan K, Nieuwint AW, van Bever Y. Recombination in a balanced complex translocation of a mother leading to a balanced reciprocal translocation in the child. Review of 60 cases of balanced complex translocations. Hum Genet. 1997;99(6):806–15.
8. Wang J, Wang D, Yin Y, Deng Y, Ye M, Wei P, et al. Assessment of Combined Karyotype Analysis and Chromosome Microarray Analysis in Prenatal Diagnosis: A Cohort Study of 3710 Pregnancies. Genet Res (Camb). 2022;2022:6791439.
9. Dong Z, Jiang L, Yang C, Hu H, Wang X, Chen H, et al. A robust approach for blind detection of balanced chromosomal rearrangements with whole-genome low-coverage sequencing. Hum Mutat. 2014;35(5):625–36.
10. Dong Z, Qian J, Law T, Chau M, Cao Y, Xue S, et al. Mate-pair genome sequencing reveals structural variants for idiopathic male infertility. Hum Genet. 2023;142(3):363–77.
11. Richards S, Aziz N, Bale S, Bick D, Das S, Gastier-Foster J, et al. Standards and guidelines for the interpretation of sequence variants: a joint consensus recommendation of the American College of Medical Genetics and Genomics and the Association for Molecular Pathology. Genet Med. 2015;17(5):405–24.
12. Dong Z, Wang H, Chen H, Jiang H, Yuan J, Yang Z, et al. Identification of balanced chromosomal rearrangements previously unknown among participants in the 1000 Genomes Project: implications for interpretation of structural variation in genomes and the future of clinical cytogenetics. Genet Med. 2018;20(7):697–707.
13. Ballarati L, Recalcati MP, Bedeschi MF, Lalatta F, Valtorta C, Bellini M, et al. Cytogenetic, FISH and array-CGH characterization of a complex chromosomal rearrangement carried by a mentally and language impaired patient. Eur J Med Genet. 2009;52(4):218–23.
14. Schluth-Bolard C, Delobel B, Sanlaville D, Boute O, Cuisset JM, Sukno S, et al. Cryptic genomic imbalances in de novo and inherited apparently balanced chromosomal rearrangements: array CGH study of 47 unrelated cases. Eur J Med Genet. 2009;52(5):291–6.
15. Gijsbers AC, Lew JY, Bosch CA, Schuurs-Hoeijmakers JH, van Haeringen A, den Hollander NS, et al. A new diagnostic workflow for patients with mental retardation and/or multiple congenital abnormalities: test arrays first. Eur J Hum Genet. 2009;17(11):1394–402.
16. Shaw-Smith C, Redon R, Rickman L, Rio M, Willatt L, Fiegler H, et al. Microarray based comparative genomic hybridisation (array-CGH) detects submicroscopic chromosomal deletions and duplications in patients with learning disability/mental retardation and dysmorphic features. J Med Genet. 2004;41(4):241–8.
17. Kline AD, Griffin CA, Haddadin MH, Chudoba I, Morsberger LA, Hawkins AL, et al. A de novo complex karyotype with two independent balanced

translocations and a double inversion of chromosome 6 presenting with multiple congenital anomalies. Am J Med Genet A. 2004;129A(2):124–9.
18. Zhang J, Wu Y. SVseq: an approach for detecting exact breakpoints of deletions with low-coverage sequence data. Bioinformatics. 2011;27(23):3228–34.
19. Pitel BA, Zuckerman EZ, Baughn LB. Mate Pair Sequencing: Next-Generation Sequencing for Structural Variant Detection. Methods Mol Biol. 2023;2621:127–49.
20. Mantere T, Neveling K, Pebrel-Richard C, Benoist M, van der Zande G, Kater-Baats E, et al. Optical genome mapping enables constitutional chromosomal aberration detection. Am J Hum Genet. 2021;108(8):1409–22.
21. Dong Z, Yan J, Xu F, Yuan J, Jiang H, Wang H, et al. Genome Sequencing Explores Complexity of Chromosomal Abnormalities in Recurrent Miscarriage. Am J Hum Genet. 2019;105(6):1102–11.
22. Ou J, Yang C, Cui X, Chen C, Ye S, Zhang C, et al. Successful pregnancy after prenatal diagnosis by NGS for a carrier of complex chromosome rearrangements. Reprod Biol Endocrinol. 2020;18(1):15.
23. Kalscheuer VM, Tao J, Donnelly A, Hollway G, Schwinger E, Kübart S, et al. Disruption of the serine/threonine kinase 9 gene causes severe X-linked infantile spasms and mental retardation. Am J Hum Genet. 2003;72(6):1401–11.
24. Kleinjan DJ, van Heyningen V. Position effect in human genetic disease. Hum Mol Genet. 1998;7(10):1611–8.
25. Feuk L, Carson AR, Scherer SW. Structural variation in the human genome. Nat Rev Genet. 2006;7(2):85–97.
26. Christina H, Nete MN, Lusine NP, Asli S, Ryan LC, Chelsea L, et al. Risks and Recommendations in Prenatally Detected De Novo Balanced Chromosomal Rearrangements from Assessment of Long-Term Outcomes. Am J Hum Genet. 2018;102(6):1090–103.
27. Ruiz C, Grubs RE, Jewett T, Cox-Jones K, Abruzzese E, Pettenati MJ, et al. Prenatally diagnosed de novo apparently balanced complex chromosome rearrangements: two new cases and review of the literature. Am J Med Genet. 1996;64(3):478–84.
28. Baptista J, Mercer C, Prigmore E, Gribble SM, Carter NP, Maloney V, et al. Breakpoint mapping and array CGH in translocations: comparison of a phenotypically normal and an abnormal cohort. Am J Hum Genet. 2008;82(4):927–36.
29. Bisgaard AM, Kirchhoff M, Tümer Z, Jepsen B, Brøndum-Nielsen K, Cohen M, et al. Additional chromosomal abnormalities in patients with a previously detected abnormal karyotype, mental retardation, and dysmorphic features. Am J Med Genet A. 2006;140(20):2180–7.
30. Weise A, Rittinger O, Starke H, Ziegler M, Claussen U, Liehr T. De novo 9-break-event in one chromosome 21 combined with a microdeletion in 21q22.11 in a mentally retarded boy with short stature. Cytogenet Genome Res. 2003;103(1–2):14–6.

Publisher's Note